Effects of Reactive Interlayers in Magnetic Pulse Welding

J. Bellmann[1,2*], J. Lueg-Althoff[3], S. Schulze[2], S. Gies[3], E. Beyer[1,2], A. E. Tekkaya[3]

[1] Institute of Manufacturing Technology, TU Dresden, Germany
[2] Fraunhofer Institute for Material and Beam Technology IWS, Dresden, Germany
[3] Institute of Forming Technology and Lightweight Components, TU Dortmund, Germany
* Corresponding author. E-mail address: Joerg.bellmann@tu-dresden.de

Abstract

Surface coatings affect the joint formation in magnetic pulse welding processes (MPW). Two types of coatings were identified in former studies. Anodized layers, for instance, are detrimental for the weld formation if they are not removed before or during welding. Contrastingly, a nickel layer on a steel parent part was found to be advantageous since it increased the weld seam length when it was impacted by an aluminum flyer. This paper gives insights into the welding mechanism with nickel coatings during MPW and explains one reason for the improved weld formation.

Metallographic analyses showed that the coating is evidently not fractured, but an interlayer between aluminum and nickel is formed. Scanning electron microscopy and energy dispersive X-ray spectroscopy revealed that nickel and aluminum have interacted. The energy release rate of the exothermic reaction is higher than the reaction of aluminum with steel in direct contact. Since all other parameters were kept constant, it is assumed that the additional heat of the nickel-aluminum reaction promotes the welding effect, especially at positions with lower impact pressures. This effect, for instance, enables a significant reduction of the required impact energy for MPW. The formation of the interaction zone was studied for different well defined collision conditions. A newly developed process measurement system was utilized, which records the characteristic process light emission and enables insights into the prevalent collision conditions.

Keywords

Magnetic Pulse Welding, Welding Windows, Interlayers

1 Introduction

Magnetic pulse welding (MPW) is a solid-state welding technology based on the high velocity collision between two metallic parts. Under proper conditions a “jet” is formed that removes oxides and contaminants from the surfaces. The cleaned surfaces are then welded together under the prevalent high pressure. The process is favorable for the production of dissimilar joints due to the low heat input that reduces the formation of intermetallic phases to an uncritical minimum. The geometrical and kinetic collision conditions that lead to successful welds are often plotted in so-called “welding windows” and depend on the mechanical and thermal properties of the involved materials. Furthermore, the surface topography of the parts determines the interface’s characteristic and strength (Geyer, 2016). Bay et al. (1994) studied the influence of strategic surface coatings during several solid-state welding processes and identified two general types of interlayers. *Passive* coatings are cracked during deformation and expose virgin base metal surfaces, which are then welded together, whereas *active* coatings act as a solder between the two base materials. Since MPW was not investigated by Bay et al. (1994), a systematic study was performed by Bellmann et al. (2016) for this process where the effects of different types and thicknesses of coatings were analyzed. The major part of the interlayers was *passive* and affected the welding result in a detrimental way. For example, the jetting effect was not able to remove a 5 µm anodized layer from an aluminum part and thus welding was prohibited with a radial impact velocity of 250 m/s. Only when the impact velocity was increased up to 400 m/s, the anodized layer was removed completely and a sound weld was achieved. In contrast to that, *active* coatings stay in the weld zone and take part in the actual bond formation. Yablochnikov (2006) suggests a soft aluminum alloy like EN AW-1100 as a transition layer with a thickness of 0.3 to 1 mm for enhancing the bond between a strong aluminum alloy and steel. The underlying effect is not described by the author, but a similar transition material is used in explosive welding, too (Czechowski, 2004). Maybe, the amount of plastic deformation is increased with one soft joining partner and thus more virgin base metal surfaces are exposed. Bellmann et al. (2016) found that a 5 µm interlayer of nickel enables MPW between aluminum and steel at positions where the pressure is comparatively low and welding would not be possible in direct contact. The results were reproducible and allow for an energy reduction during MPW with positive effects on the process efficiency (Bellmann et al., 2017a) and lifetime of the tool coils. Interestingly, the nickel layer is not fractured, the welding interface is almost smooth and the amount of plastic deformation is small compared to the aluminum interlayer described by Czechowski (2004). Since neither the duration nor the amount of the interface pressure was changed by the coating, the temperature as the third important parameter for welding processes must have been influenced. It is a well-known phenomenon that nickel and aluminum can react exothermic. This effect is used for example as a heat source within reactive multi layers for various joining processes (Leifert et al., 2014). Marya and Marya (2004) stated for MPW of aluminum to copper that the intermetallic phase (IMP) formation is an internal source of heat. Extensive formation of IMP increases the risk of voids, pores and local cracking and should therefore be prevented, for example by

decreasing the effective impact energy (Stern et al., 2014). In this paper, the *controlled* intermetallic phase formation between nickel and aluminum is utilized as an additional heat source in the joining zone and the *positive* effect on the MPW process is analyzed. Therefore, the interaction at the welding interfaces between material combinations with different heat formation levels (Ni-Al and Steel-Al) are studied and compared for two different collision conditions.

2 Experimental Design

The material combination aluminum EN AW-6060 (T66) and steel C45 (1.0503) was chosen in order to ensure the comparability with former studies (Bellmann et al., 2016; Bellmann et al., 2017a). The chemical compositions are given in Seeberger (2016) and Salzgitter Flachstahl GmbH (2011), respectively. The parent parts were used in normalized state with polished surfaces (Ra = 1 µm). The geometrical setup of the coil and the parts is depicted in **Fig. 1**. The single turn coil was made of CuCrZr alloy (2.1293) with an inner diameter of 41 mm. The characteristics of the pulse generator are given by Bellmann et al. (2017b). The steel parts were coated with 6.1 µm nickel in chemical processes before joining. The nickel coating contains up to 15 atomic percent of phosphor. Selected physical properties of the coating are compared with the flyer and parent material in **Table 1**.

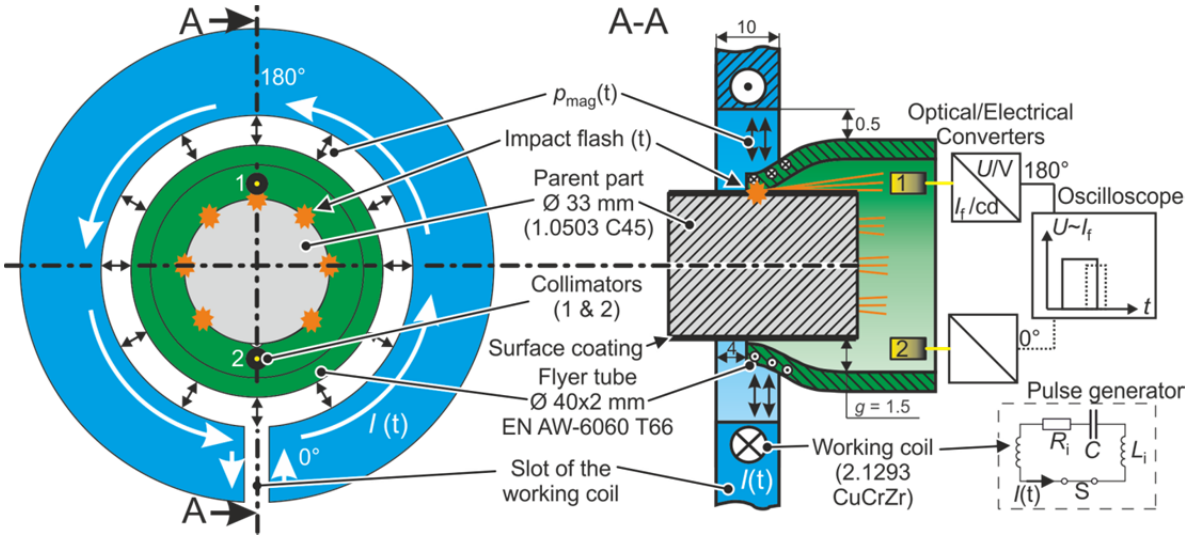

Figure 1: *Experimental setup (all values in mm)*

	Aluminum	Iron	Nickel
Melting temperature [°C]	659	1536	1455
Heat conductivity [$Wm^{-1}K^{-1}$]	204	81	59
Specific heat capacity [$Jkg^{-1}K^{-1}$]	940	470	450
Vickers hardness measured at the samples before joining	(87±3) HV0.1	(237±18) HV0.1	~520 HV0.05

Table 1: *Selected physical properties of aluminum, iron and nickel (Fischer, 2008)*

All experiments were carried out for the charging energy levels 5.8 and 8.0 kJ and with constant dimensions and positions as depicted in Fig. 1. The corresponding tool coil current was measured for each trial using a Rogowski current probe CWT 3000 B from Power Electronic Measurements Ltd. It was 426 kA ± 11 kA for the lower and 485 kA ± 5 kA for the higher energy level, respectively. The set of experiments was split into two parts. Within the first batch of experiments, the collision conditions after the initial impact of the flyer's edge were determined with the method presented by Bellmann et al. (2017b). Therefore, the collision times at two specific points along the weld front propagation were evaluated by recording the intensity of the high velocity impact flash. The optical signals were collimated at the inner circumference of the flyer tube and transmitted with polymeric optical fibers (POF, diameter 1 mm, length 7 m, by Telegaertner Geraetebau GmbH, Germany) to phototransistors. These acted as optical/ electrical converters and generated signals that were timed to the current signal from the tool coil on the oscilloscope. The measuring device recorded the light intensities at *two* positions within *one* joining experiment, see Fig. 1. The second batch of experiments covered joining trials with uncoated and nickel-coated parent parts on both energy levels.

The weld quality was checked by manual peel testing at the position of the coil's slot (0°) and at the opposite direction (180°). Therefore, strips of the flyer material with a width of approximately 6 mm were cut and bent radially. When welding was obtained, the weld seam was able to withstand a tension force normal to the weld seam or a separation in the aluminum base material of the strip occurred (crack according to classification P1024 in DIN EN ISO 6520-2 (2013)). In the case of unsuccessful welding, the strips were separated from the parent (according to classification P401/P403 in DIN EN ISO 6520-2). Metallographic analyses were done at polished cross sections at the position opposite to the coil's slot (180°). The length of the formed area, the beginning and length of the weld seam as well as the height of possible waves were determined. Selected samples underwent scanning electron microscopy (SEM) and energy dispersive X-ray spectroscopy (EDS) in order to identify the element distribution perpendicular to the weld interface. Therefore, line scans were performed with an integration width of 5 to 10 µm, see **Fig. 5a**.

3 Results and Discussion

3.1 Analysis of the Collision Conditions and Welding Results

The first set of experiments was performed in order to determine the axial and radial velocity components of the oblique impact, which are defined in **Fig. 2a** as v_c and $v_{i,r}$, respectively. Therefore, the setup depicted in **Fig. 2b** was utilized to measure the flash appearance times at two specific points along the weld front propagation by recording the intensity of the high velocity impact flash at two locations around the circumference. In every experiment, the first contact between flyer and parent occurred at the 180° position. This is typical for this kind of joining setup since the magnetic pressure and thus the acceleration is reduced near the slot.

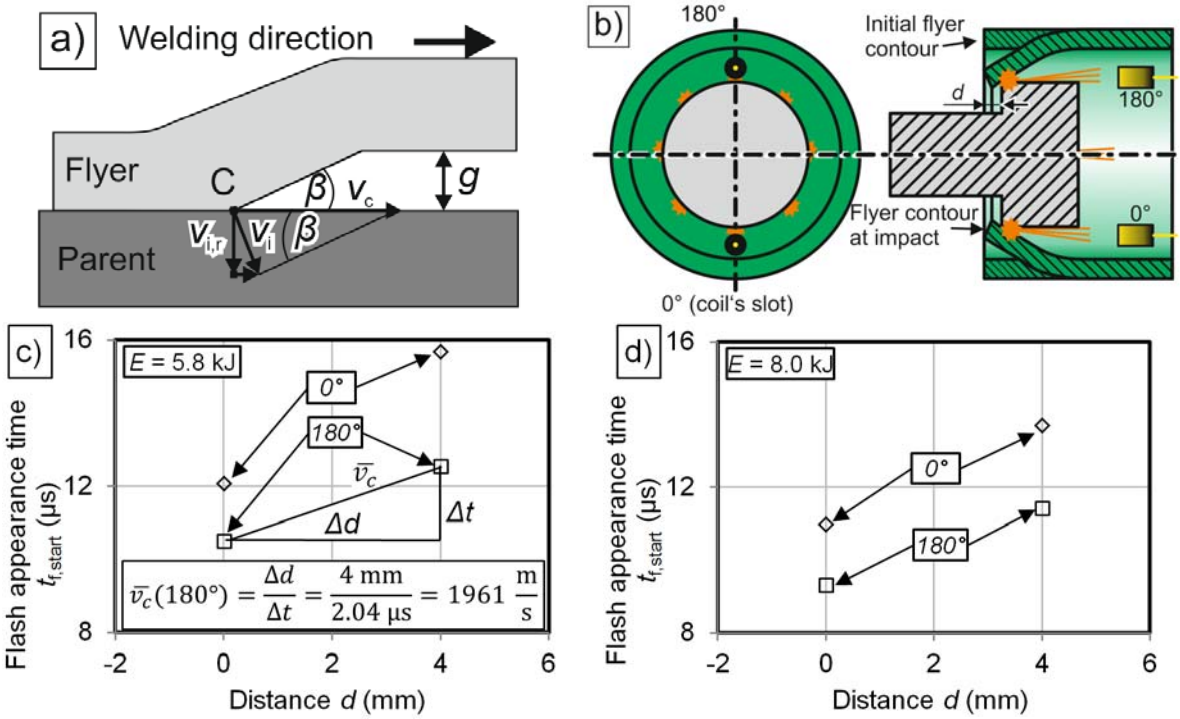

Figure 2: *a) Velocity components at the collision point C b) experimental setup with targeted variation of distance d for measurement of the flash appearance times and calculation of the mean collision front velocity* $\overline{v_c}$ *for c) 5.8 kJ and d) 8.0 kJ charging energy*

Based on the flash appearance times $t_{f,start}$, the mean collision front velocity $\overline{v_c}$ can be calculated as demonstrated in **Fig. 2c**. From previous work it is known that v_c varies over the first millimeters after the impact (Bellmann et al., 2017b). This variation is not considered here in order to focus on the comparison between both energy levels and the influence of the surface coatings. For the calculation of the prevalent initial *radial* impact velocities $v_{i,r}$, a steady flyer acceleration in radial direction is assumed. With the joining gap being g = 1.5 mm (see Fig. 1) and the delay between the collision time and the flash appearance time of about 0.5 µs (Bellmann et al., 2017b), the radial flyer velocity at the time of the initial impact can be calculated. The collision conditions and the welding results are shown in **Table 2**. A charging energy of 5.8 kJ was not sufficient to produce a circumferential weld seam between uncoated steel parent parts and the aluminum tube. Probably, the combination of a comparatively slow impact velocity and a low collision front velocity lead to the non-welded region at the position of the coil's slot (0°). Changing the energy to 8 kJ increased both velocity components significantly and enabled a circumferential weld.

Charging energy *E*	5.8 kJ		8.0 kJ	
Position	**180°**	**0°**	**180°**	**0°**
Mean collision front velocity $\overline{v_c}$ for the first four millimetre after impact [ms^{-1}]	1961	1111	2410	1471
Initial radial impact velocity $v_{i,r}$ [ms^{-1}]	299	259	340	286
Welded	yes	no	yes	yes

Table 2: *Mean collision front velocities* $\overline{v_c}$ *, initial radial impact velocities* $v_{i,r}$ *based on a steady acceleration and welding results for two energy levels with uncoated parent parts*

3.2 Characterization of the Weld Interface

The second set of experiments focused on the influence of the nickel coating on the weld seam formation. Therefore, optical micrographs of the cross sections at the 180° position were taken from each sample and compared with the uncoated ones. The characteristic values are defined in **Fig. 3b** and listed in **Table 3** for both energy levels. As the results show, the flyer forming is influenced by the applied energy but not by the coating. Thus, the most important welding parameters pressure, time and temperature are assumed to be equal for each energy level. This allows a direct comparison of the uncoated and nickel-coated samples.

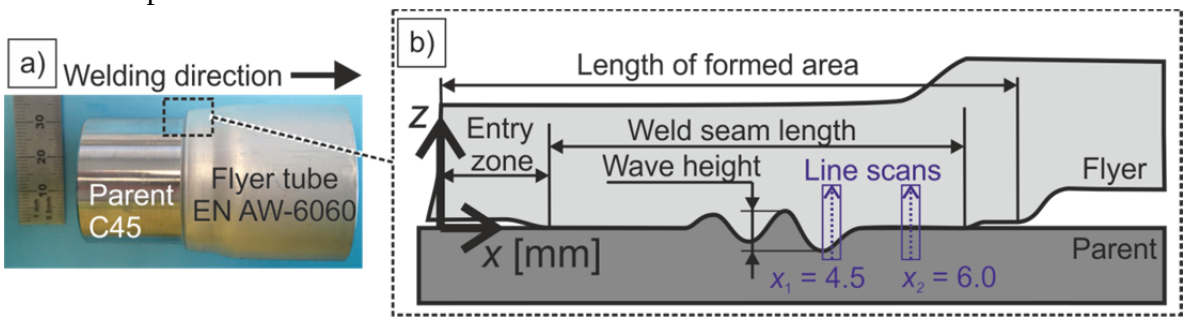

Figure 3: *a) Joined Sample with location of the cross section at 180°, b) schematic cross section with characteristic values of the weld seam*

Charging energy *E*	5.8 kJ		8.0 kJ	
$\overline{v_c}$	1961 ms^{-1}		2410 ms^{-1}	
Coating	**-**	**Ni**	**-**	**Ni**
Length of formed area [mm]	7.6	7.5	8.1	8.2
Length of entry zone [mm]	0.9	0.8	1.3	0.7
Weld seam length [mm]	3.6	5.8	3.9	7.0
Maximum wave height [µm]	9	4	10	6

Table 3: *Influence of the charging energy and coating on the weld seam characteristic at the 180° position*

The application of a nickel interlayer increases the weld seam length and produces a sound joint even at *x*-positions that were not welded in the uncoated sample. This effect is intensified by a higher energy input. **Fig. 4b** shows the detailed optical micrograph from the location, which was welded at the nickel-coated sample but not welded at the uncoated sample.

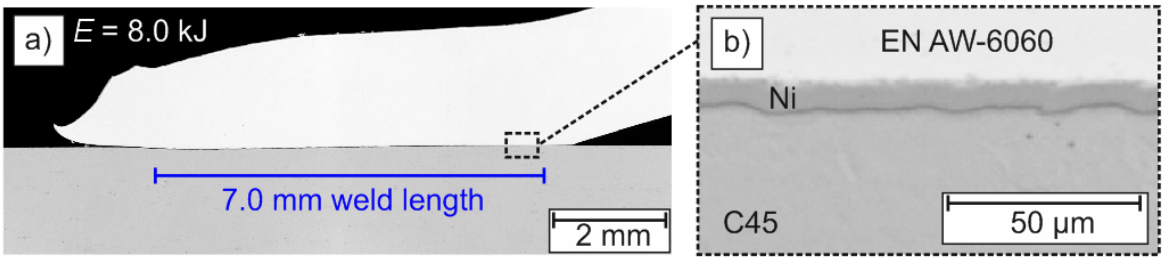

Figure 4: *Optical micrographs of the cross section from the nickel-coated sample with a) marked weld length and b) end of the weld seam*

At the position x_1 of the uncoated sample, the wave formation is distinctly developed and the areas of the interaction between iron and aluminum are concentrated in "pockets" between the waves, see **Fig. 5a**. There is a strong gradient in the element distribution perpendicular to the interface for z < 5 µm as shown in **Fig. 5c**. By the way of contrast, the nickel-coated sample in **Fig. 5b** shows an almost continuous layer without significant wave formation. It consists of 40 to 50 atomic percent aluminum and 60 to 50 atomic percent nickel, respectively.

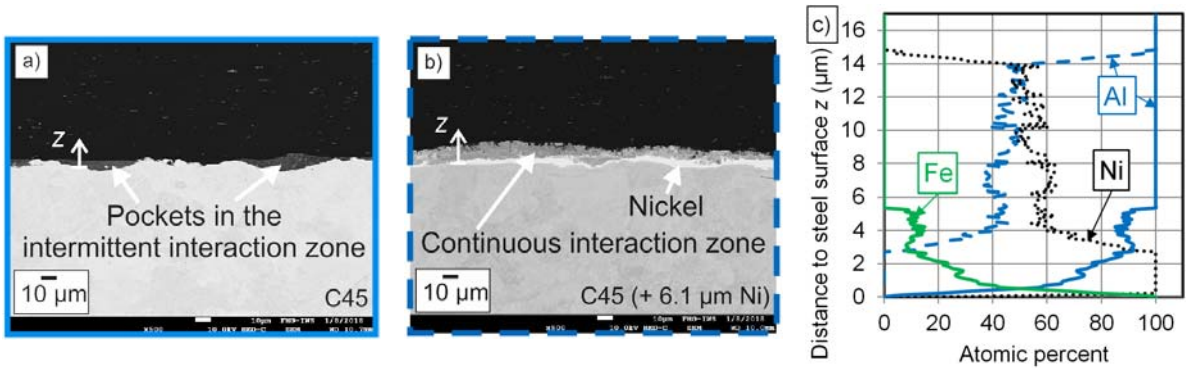

Figure 5: *SEM micrographs at x_1 with a) uncoated and b) nickel-coated parent part c) comparison of EDS line scans perpendicular to the weld interface (nickel-coated sample with dotted lines, E = 8.0 kJ)*

The different characteristics of the weld interfaces could be attributed to the lower hardness of the steel surface compared to the nickel coating (see Table 1), which facilitates wave formation. Nevertheless, it does not explain the extension of the weld seam at the nickel-coated sample. Since the thermal properties of nickel and iron are very similar, the temperature conditions on the parent surface affecting possible surface melting are almost

identical in the moment just before the contact, too. It seems likely that the activated materials of the flyer and parent surfaces react, when they are pressed together. The reaction between aluminum and nickel is exothermic with a maximum energy release rate of 60 kJmol^{-1} (Sikka, 1994). The reaction of iron with aluminum does not exceed 30 kJmol^{-1} (Sikka, 1994) and thus less energy is available for the bond formation compared to the MPW process of aluminum on nickel. The additional heat of the exothermic Ni-Al-reaction could be an explanation for the extended weld zone. To get deeper insights into the processes at the interface, the width and chemical composition of the nickel-aluminum interaction zones were analyzed and compared for different positions and energy levels in **Fig. 6**.

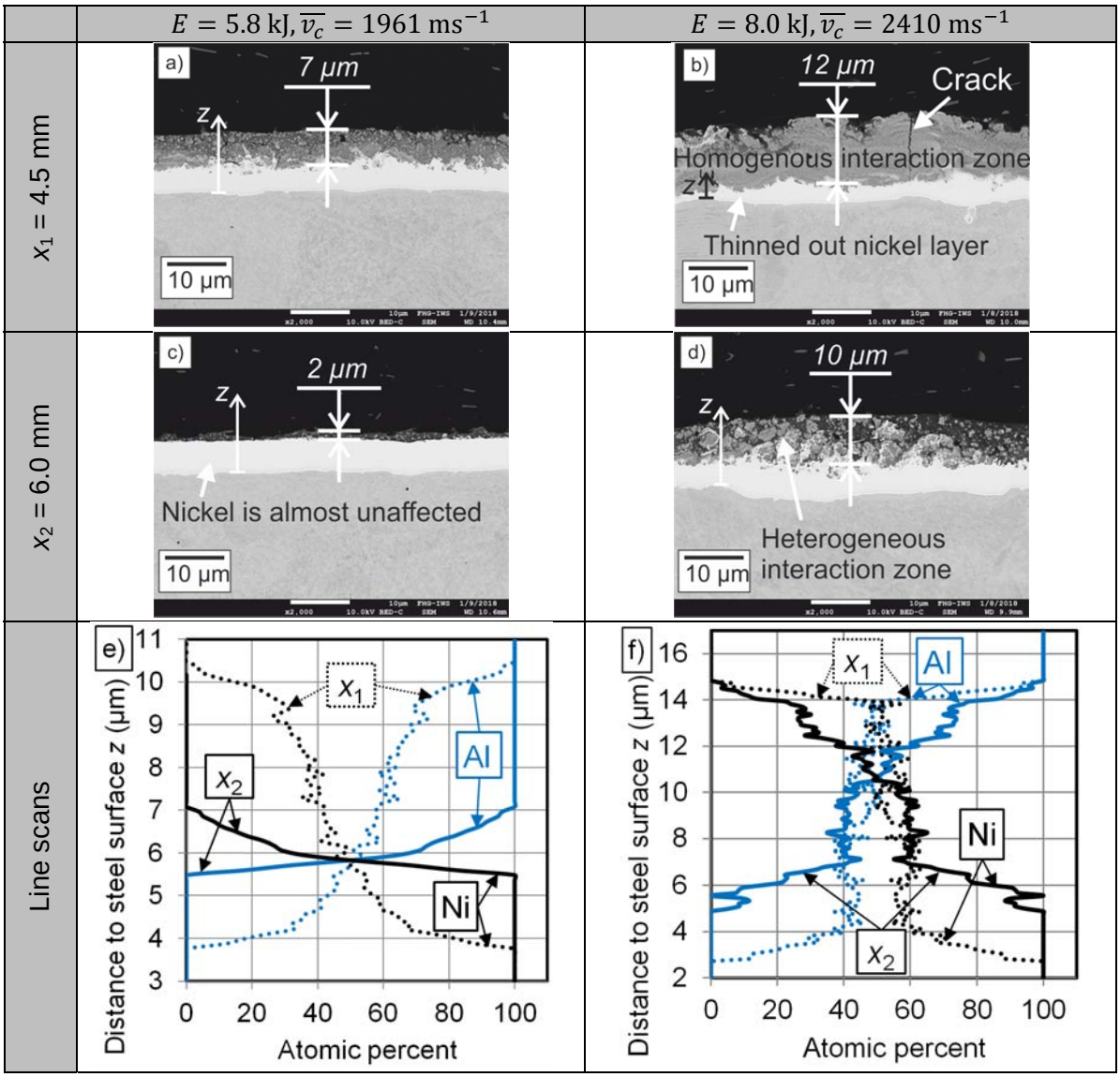

Figure 6: *a) - d) SEM micrographs for nickel-coated samples on two different energy levels and positions e), f) EDS line scans across the interaction zones*

For the lower energy level and lower interface pressure at x_2, the thickness of the interaction zone is 2 µm and the element gradient is quite harsh, see **Fig. 6c and e**. Probably, only a small share of surface material was activated before the impact and thus less material participated in the reaction compared to the position x_1 with 8 kJ charging energy (**Fig. 6b**). Here, the radial and axial velocity components were higher (approx. 13 and 23 %, respectively) and the original nickel layer has been thinned out significantly. The interaction zone is 12 µm thick and shows a homogeneous structure and element distribution (**Fig. 6f**). Obviously, more surface material participated in the Ni-Al-reaction, leading to a higher heat development. Probably as a consequence of the increased heating, solidification shrinkage lead to the cracks which are indicated in Fig. 6b and which were also reported by Stern et al. (2014). They can be avoided by limiting the activation energy, the amount of material participating in the exothermic reaction and thus the heat development. **Fig. 6d** represents these conditions at the x_2-position. Here, the interaction zone has a lowered thickness of 10 µm and a heterogeneous structure without any cracks.

4 Conclusion and Outlook

When aluminum is magnetic pulse welded on steel, the seam length can be enlarged using a nickel interlayer. Nickel acts as an *active* coating, since it is not removed before welding. It takes part in the bond formation itself while a continuous interaction zone between aluminum and nickel is formed. It is assumed that in this zone, an exothermic reaction takes place with a higher energy release rate than iron and aluminum exhibit in direct contact. Probably, the additional thermal energy supports the weld formation and thus welding is possible even at areas that were not welded without the nickel interlayer.

The positive effect of nickel was observed for two different energy levels with distinct different collision conditions. It was also found that the risk of cracks increases at positions with high energy input. The targeted manipulation of the collision conditions by an adapted joining setup is therefore essential to establish an optimum welding regime between aluminum flyers and nickel coated parent parts. The results indicate that even a nickel coating with a thickness below 6.1 µm is sufficient. This would lead to lower costs and reduced time for the application of the coating. The tuning of the nickel coating to the prevalent collision conditions will be part of future work.

Acknowledgments

This work is based on the results of subproject A1 of the priority program 1640 (“joining by plastic deformation”); the authors would like to thank the German Research Foundation (DFG) for its financial support. Furthermore, the effort for the sample preparation and SEM and EDS analysis at Fraunhofer IWS Dresden is greatly acknowledged.

References

Bay, N., Zhang, W., Jensen, S.S., 1994. *The application of strategic surface coatings to improve bonding in solid phase welding*. The International Journal for the Joining of Materials 6, pp. 47–57.

Bellmann, J., Beyer, E., Lueg-Althoff, J., Gies, S., Tekkaya, A.E., Schettler, S., Schulze, S., 2017a. *Targeted Weld Seam Formation and Energy Reduction at Magnetic Pulse Welding (MPW)*. Biuletyn Instytutu Spawalnictwa 2017, pp. 91–102. doi:10.17729/ebis.2017.5/10.

Bellmann, J., Lueg-Althoff, J., Göbel, G., Gies, S., Beyer, E., Tekkaya, A.E., 2016. Effects of Surface Coatings on the Joint Formation During Magnetic Pulse Welding in Tube-to-Cylinder Configuration, In: Tekkaya, A.E., Kleiner, M. (Eds.) ICHSF 2016. Proceedings of the 7th International Conference on High Speed Forming, pp. 279–288.

Bellmann, J., Lueg-Althoff, J., Schulze, S., Gies, S., Beyer, E., Tekkaya, A.E., 2017b. *Measurement of Collision Conditions in Magnetic Pulse Welding Processes.* Journal of Physical Science and Application 7, pp. 1–10. doi:10.17265/2159-5348/2017.04.001.

Czechowski, M., 2004. *Stress corrosion cracking of explosion welded steel-aluminum joints*. Materials and Corrosion 55, pp. 464–467. doi:10.1002/maco.200303771.

DIN Deutsches Institut für Normung e.V., Dezember 2013. Schweißen und verwandte Prozesse – Einteilung von geometrischen Unregelmäßigkeiten an metallischen Werkstoffen -Teil 2: Pressschweißungen, [accessed 06 September 2016].

Fischer, U., 2008. Tabellenbuch Metall, 44th edn., Europa Lehrmittel, Haan-Gruiten

Geyer, M.H., 2016. Magnetpulsschweißen von Aluminium und Stahl: Einflüsse der Topografie auf Verbindungsausbildung und Festigkeit, 1st edn., Shaker, Herzogenrath

Leifert, A., Mondin, G., Dörfler, S., Hampel, S., Kaskel, S., Hofmann, E., Zschetzsche, J., Pflug, E., Dietrich, G., Rühl, M., Braun, S., Schädlich, S., 2014. *Fabrication of Nanoparticle-Containing Films and Nano Layers for Alloying and Joining*. Advanced Engineering Materials 16, pp. 1264–1269.doi:10.1002/adem.201400196.

Marya, M., Marya, S., 2004. *Interfacial microstructures and temperatures in aluminium–copper electromagnetic pulse welds*. Science and Technology of Welding and Joining 9, pp. 541–547.

Salzgitter Flachstahl GmbH, 2011. C45 Vergütungsstähle, http://www.salzgitter-flachstahl.de/fileadmin/mediadb/szfg/informationsmaterial/produktinformationen/warmgewalzte_produkte/deu/c45.pdf, [accessed 18 January 2018].

Seeberger, 2016. Datasheet AlMgSi (EN AW-6060), http://www.seeberger.net/_assets/pdf/werkstoffe/aluminium/de/AlMgSi.pdf, [accessed 08 September 2016].

Sikka, V.K., 1994. Melting, Casting, and Processing of Nickel and Iron Aluminides. MRS Proceedings 364, 712. doi:10.1557/PROC-364-873.

Stern, A., Shribman, V., Ben-Artzy, A., Aizenshtein, M., 2014. *Interface Phenomena and Bonding Mechanism in Magnetic Pulse Welding*. Journal of Materials Engineering and Performance 23, pp. 3449–3458. doi:10.1007/s11665-014-1143-0.

Yablochnikov, B.A., 2006. Method of magnetic pulse welding an end fitting to a driveshaft tube of a vehicular driveshaft, http://pdfstore.patentorder.com/pdf/us/435/us 7015435.pdf, [accessed 19 April 2017]